ACS APPLIED MATERIALS & INTERFACES

Research Article

www.acsami.org

Facile Preparation of Paclitaxel Loaded Silk Fibroin Nanoparticles for Enhanced Antitumor Efficacy by Locoregional Drug Delivery

Puyuan Wu,[†] Qin Liu,[†] Rutian Li,[†] Jing Wang,[‡] Xu Zhen,[‡] Guofeng Yue,[§] Huiyu Wang,[∥] Fangbo Cui,[†] Fenglei Wu,[∥] Mi Yang,[†] Xiaoping Qian,[†] Lixia Yu,[†] Xiqun Jiang,[‡] and Baorui Liu*[,†]

[†]The Comprehensive Cancer Centre of Drum Tower Hospital, Medical School of Nanjing University, Clinical Cancer Institute of Nanjing University, 321 Zhongshan Road, Nanjing 210008, China

[‡]Laboratory of Mesoscopic Chemistry and Department of Polymer Science, Engineering College of Chemistry & Chemical Engineering, Nanjing University, Nanjing 210093, China

[§]Nanjing Medical University, 140 Hanzhong Rd, Nanjing 210029, China

[∥]The Comprehensive Cancer Center of Drum Tower Hospital, Nanjing Medical University, 321 Zhongshan Rd, Nanjing 210008, China

S *Supporting Information*

ABSTRACT: Non-toxic, safe materials and preparation methods are among the most important factors when designing nanoparticles (NPs) for future clinical application. Here we report a novel and facile method encapsulating anticancer drug paclitaxel (PTX) into silk fibroin (SF), a biocompatible and biodegradable natural polymer, without adding any toxic organic solvents, surfactants or other toxic agents. The paclitaxel loaded silk fibroin nanoparticles (PTX-SF-NPs) with a diameter of 130 nm were formed in an aqueous solution at room temperature by self-assembling of SF protein, which demonstrated mainly silk I conformation in the NPs. In cellular uptake experiments, coumarin-6 loaded SF NPs were taken up efficiently by two human gastric cancer cell lines BGC-823 and SGC-7901. In vitro cytotoxicity studies demonstrated that PTX kept its pharmacological activity when incorporating into PTX-SF-NPs, while SF showed no cytotoxicity to cells. The in vivo antitumor effects of PTX-SF-NPs were evaluated on gastric cancer nude mice exnograft model. We found that locoregional delivery of PTX-SF-NPs demonstrated superior antitumor efficacy by delaying tumor growth and reducing tumor weights compared with systemic administration. Furthermore, the organs of mice in NP treated groups didn't show obvious toxicity, indicating the in vivo safety of SF NPs. These results suggest that SF NPs are promising drug delivery carriers, and locoregional delivery of SF NPs could be a potential future clinical cancer treatment regimen.

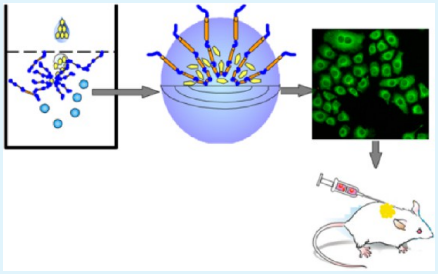

KEYWORDS: *silk fibroin, nanoparticle, paclitaxel, locoregional chemotherapy, in vivo*

INTRODUCTION

Nanoparticle therapeutics, a promising treatment modality in oncology application,[1] has been proved to enhanced the efficacy of anticancer agents.[2,3] However, it is important to notice that problems related with safe and efficient in vivo administration of most nanoparticles (NPs) were still unsolved, such as cytotoxic materials,[4] toxic solvent or surfactant addition, harsh fabrication conditions unsuitable for bioactive drugs, immunogenicity for repeated administration,[5] etc. NPs with good biocompatibility and green chemical processability for future clinical applications were desirable.

Silk fibroin (SF) derived from *Bombyx mori* is a protein proved to be of excellent biocompatibility and in vivo degradability.[6−8] SF is the main structure protein of silk, which is used to produce textile and surgical sutures. It has been reported that the immunoresponse to silk sutures is associated with sericin, a glue-like protein holding the fiber-like SF together to be silk. Nevertheless, as the other component of sutures, SF is low immunogenicity.[9] SF is processable and has been fabricated into various formulations for regeneration engineering study and drug delivery including fibers, films, 3D-scaffods, gels, etc.[10] The SF scaffolds and matrixes demonstrate good biocompatibility with cells and tissues in vitro and in vivo.[11,12] Furthermore, the degradation of SF protein could be tuned by SF crystallinity and structure.[6] Thus, SF is a promising candidate for drug carrier design.

Recently, several methods are available for SF NP and microparticle fabrication, such as PVA blend film,[13] phase separation in salt solution,[14] and ethanol addition and freezing.[15−18] However, preparing drug loaded SF NPs with a diameter less than 200 nm is still a great challenge. Water-miscible organic solvent methods have been reported with relative smaller particle size compared to other methods,[19−22] but excessive organic solvents are toxic and unfavorable for

Received: September 14, 2013
Accepted: November 25, 2013
Published: November 25, 2013

hydrophobic drug encapsulation. Therefore, new strategies are desired to develop drug loaded SF NPs which are non-toxic and safe for future clinical use.

Locoregional anticancer drug delivery is an efficacious supplement or replace of systemic chemotherapy for inorperable malignancies or prevention of recurrence.[23] It is notable that, different from lung cancer and breast cancer, which could metastasis to many organs including brains and bones, local recurrence and peritoneal dissemination were the major metastasis and leading cause of death of gastric cancer, and metastasis out of abdomen are rather rare. Therefore, locoregional control is important for gastric cancer.[24] Paclitaxel (PTX), one of the most widely used anticancer agents, has been demonstrated activities against various solid cancer including gastric cancer.[25] However, therapeutic response of PTX is often accompanied by severe side effects, including neutropenia associated with marrow suppression and hypersensitivity reaction associated with solvent Cremophor EL.[26,27] Locoregional delivery of PTX without toxic solvent could enhance antitumor efficacy while reducing unfavorable side effects.

In the present study, we developed a novel and facile method to prepare SF NPs. Paclitaxel-silk fibroin nanoparticles (PTX-SF-NPs) were fabricated by self-assembling of SF protein in aqueous solution at room temperature without adding surfactants and excessive toxic organic solvent. The investigation outlines the characterizations of PTX-SF-NPs, in vitro toxicity against human gastric cell lines, and in vivo antitumor efficacy for systemic and locoregional gastric cancer treatment.

MATERIALS AND METHODS

2.1. Materials. Cocoons of *B. mori* silkworm were produced from Jiangsu Province, China. PTX were offered by Jiangsu Yew Pharmaceutical Co., Ltd. (Jiangsu, China). PTX injection was offered by Yangtze River Pharmaceutical Group (Jiangsu, China). Coumarin-6 (Aldrich, U.S.A.), RPMI 1640 (Gibco, USA), calf blood serum (Lanzhou Minhai Bioengineering, China), and dimethylthiazoly-2,5-diphenyltetrazolium bromide (MTT, Amersco, U.S.A.) were used as received. Acetonitrile (Merck, Germany) was of HPLC grade. Milli-Q ultra-pure water was used. All the other chemicals were of analytical grade and were used without further purification. Human gastric carcinoma cell line BGC-823 and SGC-7901 were obtained from Shanghai Institute of Cell Biology (Shanghai, China).

2.2. Silk Fibroin Purification, Sterilization, and Molecular Weight. The SF aqueous solution was prepared as previously reported[28] with mild modification. Briefly, cocoons were cut into small pieces and degummed in boiled 0.5% sodium carbonate for 30 min twice, followed by thorough wash with deionized water. After air-drying, the degummed SF was dissolved in a ternary solution (molar ratio $CaCl_2/CH_3CH_2OH/H_2O$ = 1:2:8) at 70 °C for 4 h. The resulting solution was dialysis (MWCO 14 000 Da) against deionized water for 4 days to remove salts and ethanol. After centrifuge (10 000 rpm for 15 min) and filter through 0.22 μm filter for sterilization, the SF aqueous solution (50 mg/mL) was stored at 4 °C and diluted with sterilized Milli-Q water before use. The concentration of SF solution was determined by weighting the residual solid after drying a predetermined volume of solution at 60 °C for 24 h. The molecular weight range of SF extracted was investigated by SDS-PAGE with 12% separation gel and 5% condensing gel,[29] followed by coomassie brilliant blue R-250 staining.[20]

2.3. Paclitaxel Silk Fibroin Nanoparticle Preparation. PTX-SF-NPs were formed in aqueous solution by adding PTX solution into aqueous SF solution. Typically, 5 mg/mL SF solution was prepared, to which 5 mg of PTX in ethanol was introduced dropwise under constant stirring. The resulting milky bluish solution was filtered to exclude large aggregates and centrifuged at 12 000 rpm for 30 min. The pellets were washed twice and suspended in saline using an ultrasound processor SONICS Vibra-cell VCX130 (Sonics & Materials, Inc., U.S.A.) at 20% amplitude for 2 s. All of the steps were operated in a super clean bench to keep sterilized.

2.4. Nanoparticle Characterization. *2.4.1. Particle Size and ζ Potential.* PTX-SF-NPs particle size and polydispersity (PDI) were measured by dynamic light scattering (DLS) with a Brookheaven BI-900AT instrument (Brookheaven Instruments Corporation, U.S.A.). ζ potential was determined by a ζ potential analyzer (Brookheaven Instruments Corporation, U.S.A.). All measurements were performed at 25 °C for triplicate.

2.4.2. Morphology Study. The morphology study of PTX-SF-NPs was conducted under a JEM-100s (Japan) transmission electron microscopy (TEM). Copper wire meshes were immersed in the NP solution for seconds and air-dried before observation without staining.

2.4.3. Infrared Spectra. To investigate the conformation of SF in PTX-SF-NPs, infrared spectra were recorded with a Fourier transform infrared spectrophotometer (FTIR) (Bruker VERTEX80 V, Germany). Lyophilized regenerated silk fibroin (LSF) and degummed silk fibroin fiber (SFF) were also examined. The spectra were all recorded at a resolution of 4 cm^{-1} and were generated from 32 scans.

2.4.4. X-ray Diffraction. To determine the β-sheet structure and crystallinity of SF in PTX-SF-NPs, the X-ray diffraction (XRD) intensity curves were measured by a Rigaku Ultima III X-ray diffractometer (Rigaku Corporation, Japan). LSF and SFF were also examined. The curves were all recorded at a scanning rate of 3°/min with the scanning region of 5−45°.

2.4.5. Drug Loading Content and Encapsulation Efficiency. The drug loading content and encapsulation efficiency of PTX-SF-NPs were analyzed by an Agilent high performance liquid chromatography (HPLC) system with a Zorbax C18 column (150 mm × 4.6 mm, 5 μm, Agilent Technologies, USA). The mobile phase was acetonitrile/water (52/48, v/v). The retention time for PTX was 5.5 min at 227 nm detective wavelength. The drug loading content (DL) and encapsulation efficiency (EE) were calculated by the following equations:

$$\mathrm{DL}(\%) = \frac{\text{weight of the drug in NPs}}{\text{weight of the NPs}} \times 100\% \quad (1)$$

$$\mathrm{EE}(\%) = \frac{\text{weight of the drug in NPs}}{\text{weight of the feeding drug}} \times 100\% \quad (2)$$

2.4.6. In Vitro Paclitaxel Release of Paclitaxel-Silk Fibroin-Nanoparticles. The PTX-SF-NPs were suspended in 1 mL 0.01 M pH 7.4 phosphate buffered saline (PBS) containing 0.5% (w/v) Tween-80. The solution was placed into a dialysis bag (MWCO = 14 000 Da) and immerged into 40ml 0.01M pH7.4 PBS containing 0.5% Tween-80 at 37°C in a constant temperature shaker for 100h. At predetermined time points, a volume of 4 mL release medium was withdrawn and equivalent volume of fresh medium was added. The samples were extracted with dichloromethane, vacuum dried at 37°C and reconstituted with acetonitrile. The PTX in the samples were determined by HPLC as described in section 2.4.5. The calibration curve consisted of serial concentrations of PTX suspended in the release medium and extracted and reconstituted under the same condition of testing samples.

2.5. In Vitro Particle Cellular Uptake. To investigate cellular uptake of SF NPs, coumarin-6 loading SF NPs was prepared. Briefly, coumarin-6 was dissolved in acetone and added into 5 mg/mL SF solution drop wise. The resulting solution was agitated for 3 h to remove acetone. The coumarin-6 SF NPs was filtered, centrifuged at 12 000 rpm for 30 min and suspended in saline. For cellular uptake studies, human gastric cancer cell lines BGC-823 and SGC-7901 were seeded onto glass covers placed in 6-well plates at a density of 3×10^5 cell per well with PRMI 1640 supplemented with 10% calf serum. After incubated at 37°C with 5% CO_2 for 24h, the culture medium were added with 200 μL of coumarin-6 SF NPs (equaled to 6.5 μg/mL in medium) and incubated for 2 h. The glass covers were washed with PBS for three times and observed under a fluorescence microscopy (Olympus, Japan) with wide band blue excitation.

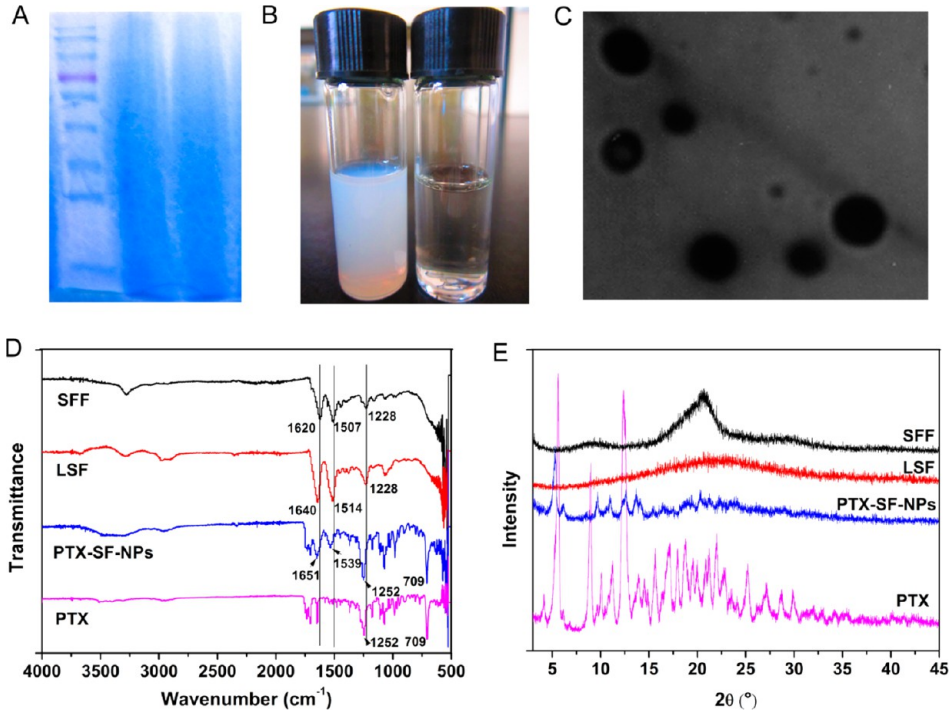

Figure 1. Fabrication and characterization of PTX-SF-NPs. (A) SDS-PAGE of SF dissolved by $CaCl_2$·CH_3CH_2OH·H_2O ternary system. The protein markers from up to down: 170, 130, 100, 70, 55, 40, 35, 25, and 15 kDa. (B) Formation of PTX-SF-NPs. Left, SF solution adding PTX ethanol solution. Right, SF solution adding equivalent ethanol. (C) TEM of PTX-SF-NPs. (D) FTIR of PTX-SF-NPs. (E) XRD of PTX-SF-NPs. SFF and LSF were recorded as control of silk II and silk I conformation, respectively.

2.6. In Vitro Cytotoxicity Studies. The cytotoxicity of PTX-SF-NPs against human gastric cell lines BGC-823 and SGC-7901 were determined by 3-(4,5-dimethylthiazol-2-yl)-2,5-diphenyltetrazolium (MTT) assay. Cells was seeded in 96-well plates (9600 cell per well) with PRMI 1640 supplemented with 10% calf serum and incubated at 37 °C with 5% CO_2 for 24 h. Cells were then exposed to various doses of PTX PTX-SF-NPs and SF for 48 h, followed by incubation with 20 μL of 5 mg/mL MTT for 4 h, allowing the viable cells to transform the yellow MTT to dark blue formazan. The medium were discharged and a volume of 150 μL dimethylsulfoxide (DMSO) was added to dissolve the formazan crystals. The absorption of each well was measured by an ELISA reader (ELX800 Biotek, U.S.A.) with test and reference wavelength of 490 nm and 630 nm, respectively. Cell viabilities were calculated by the following formula:

$$\text{cell viability}(\%) = \frac{\text{Abs(sample)}}{\text{Abs(control)}} \times 100\% \quad (3)$$

All the results were from three independent experiments and test in triplicate each time.

2.7. Apoptosis Study. The apoptosis of gastric cells after treatment with PTX and PTX-SF-NPs was investigated by a flow cytometry (BD FACS Atira II, BD Company, U.S.A.) with a cell apoptosis kit (Alexa Fluor 488 annexin V/Dead Cell Apoptosis Kit with Alexa Fluor 488 annexin V and PI for Flow Cytometry, Invitrogen). BGC-823 cells was seeded in 6-well plates at a density of 2 × 10^5 cell per well with PRMI 1640 supplemented with 10% calf serum and incubated at 37 °C for 24 h. After that, the medium were replaced with PTX, SF, and PTX-SF-NPs in fresh medium and incubated for 48 h. The cells were then dissociated with trypsin and washed with PBS. After adding PI and fluorescence labeled annexin V under the instruction of manufacture, the cells were analyzed by cytometry. The apoptotic cell ratio was calculated by the ratio of apoptosis cells and dead cells to total cells.

2.8. In Vivo Antitumor Efficacy on a Human Gastric Cancer Nude Mice Xenograft Model. To investigate the in vivo antitumor efficacy of PTX-SF-NPs for systemic and locoregional treatment of gastric cancers, a subcutaneous human gastric cancer BGC823 nude mice xenograft model was used. The 4-week old Balb/c nude mice were raised under specific pathogen-free (SPF) environment in compliance with guidelines set by the Animal Care Committee at Drum Tower Hospital, Nanjing, China. A volume of 0.1 mL of saline contained 2 × 10^6 BGC823 cells were injected subcutaneously into lower right axilla of the mice. When 80% of the tumors reached a volume of 100 mm^3, the mice were divided into 5 groups randomly and each group contains 6 mice. The day was designated as "Day 1". On Day 1, 4 groups of the mice were intraperitoneal (ip) treated with saline, SF (77 mg/kg, equaled to SF in PTX-SF-NPs), PTX injection (10 mg/kg PTX), and PTX-SF-NPs (10 mg/kg PTX), respectively. Mice of the last group were anaesthetized and peritumoral (pt) injected PTX-SF-NPs (10 mg/kg PTX). The treatments were carried out every 4 days for 3 times. Tumor sizes were measured every day by a vernier calipers, and tumor volumes were calculated as $V = D \times d^2/2$ (D and d were the longest and the shortest diameter of tumor in mm respectively). Relative tumor volumes were calculated by the following equation to reduce the impact of initial tumor volume differences after grouping:

$$\text{relative tumor volume} = \frac{V}{V_0} \quad (4)$$

V was the absolute tumor volume, and V_0 was the average tumor volume of the group on Day 1.

On Day 14, the mice were sacrificed. Tumors were collected for tumor weighting and hematein and eosin (H&E) staining. Hearts, lungs, livers, spleens, and kidneys were collected for H&E staining to assess the systemic toxicity of PTX-SF-NPs.

2.9. Statistical Analysis. All data were listed as mean ± sem. Statistical analysis of data was made by ANOVA or Student's t-test. It was considered significantly different if $p < 0.05$.

RESULTS AND DISCUSSION

3.1. Fabrication of Paclitaxel Silk Fibroin Nanoparticles. SF is a biomacromolecule consists of 5509 amino acids and composes a heavy chain (391 kDa) and a light chain

Table 1. Characterization of PTX-SF-NPs Fabricated by Different Silk Concentrations, Drug Feeding Ratios, and Solvents

SF (mg/mL)	SF/PTX (w/w)	solvent	solvent/water (v/v)	particle size (nm)	polydispersity	ζ potential (mV)
2	25:5	ethanol	2:100	196.6 ± 1.6	0.158 ± 0.020	−7.10
5	25:2	ethanol	2:100	176.5 ± 0.4	0.125 ± 0.017	−21.23
5	25:5	ethanol	4:100	158.4 ± 0.4	0.117 ± 0.014	−2.47
10	25:2	ethanol	4:100	175.4 ± 0.9	0.144 ± 0.027	−10.28
5	25:5	methanol	4:100	186.2 ± 3.0	0.141 ± 0.010	−2.35
5	25:5	acetone	4:100	206.7 ± 2.4	0.221 ± 0.005	−2.26

(26 kDa).[30] It has been reported that SF molecule undergo hydrolysis during degummed procedure. Similarly, in our study, SDS-PAGE showed that the regenerated SF was a mixture of polypeptides with a wide molecular distribution (Figure 1A). The solution turned milky immediately after introducing PTX ethanol solution to SF solution under stirring at ambient temperature (Figure 1B). TEM showed that PTX-SF-NPs were regular round shaped and in a diameter of 130 nm approximately (Figure 1C). However, the phenomenon was not observed by adding equivalent volume of ethanol without PTX (Figure 1B), which indicated PTX played an important role in NPs formation.

We next investigate the impact of different PTX solvents, silk concentrations, and drug feeding ratios on the formation of PTX-SF-NPs (Table 1). It had been proved that besides ethanol, methanol and acetone, both of which are water miscible solvents, could be applied as PTX solvents to fabricate PTX-SF-NPs. The diameter of PTX-SF-NPs measured by DLS were 158.4 ± 0.4, 186.2 ± 3.0, and 206.7 ± 2.4 nm for ethanol, methanol, and acetone, respectively, at the same silk concentration (5 mg/mL) and drug feeding ratio (25:5, w/w). The PDI for the three solvents were 0.117± 0.014, 0.141 ± 0.010, and 0.221 ± 0.005, respectively, and the ζ potential were similar. Both silk concentration and drug feeding ratio could affect diameter, PDI and ζ potential (Table 1). Because of the smaller size, homogenous size distribution and lower cytotoxicity of ethanol compared with the other two solvents, it was chosen for the next in vitro and in vivo experiment.

3.2. FTIR and XRD Characterization of Paclitaxel Silk Fibroin Nanoparticles. The molecular structure of SF consists of large regions of hydrophobic amino acids, separated by short hydrophilic regions. The hydrophobic domain of SF is largely repeated sequences of $(Gly-Ala-Gly-Ala-Gly-Ser)_n$. In native silk fibers, the repeated sequences organized together by hydrogen bonds, forming β-sheets, crosslinking and stabilizing silk structures. In regenerative SF solutions, random coils or α-helixes are reported to be the main structure. In some conditions, such as low pH, methanol, changes of ion strength, high shear force, SF in regenerative aqueous solutions could transform into β-sheets structure. To explore the conformation of SF in PTX-SF-NPs, FTIR and XRD were recorded. Silk fibroin fibers (SFF) and lyophilized regenerated silk fibroin (LSF) were prepared as control for silks II and I conformation, respectively.

The FTIR spectrum of PTX-SF-NPs was shown in Figure 1D. SFF with typical silk II structure had characteristic absorption bands at 1620 (amide I), 1507 (amide II), and 1228 cm^{-1} (amide III). Regenerated SF is commonly α-helix and random coil instead of β-sheets structure in aqueous solution. LSF had absorption frequencies at 1640 (amide I), 1514 (amide II), and 1228 cm^{-1} (amide III), which represent the silk I structure of regenerated SF aqueous solution, although some fractions of β-sheets could form during freezing and lyophilization process. PTX-SF-NPs had absorption at 1651 (amide I) and 1539 cm^{-1} (amide II), which were shifted from β-sheets structure and indicated a silk I or random coil conformation. Additional absorptions at 1252 and 709 cm^{-1} of PTX-SF-NPs were characteristics of PTX encapsulated in NPs, as proved by pristine PTX IR spectrum.

The XRD spectrum of PTX-SF-NPs was shown in Figure 1E. The characteristic diffraction peaks of β-sheets crystalline at 2θ = 20.19° was observed in SFF, while the typical scattering of amorphous SF with a low and broad peak at around 2θ = 21.68° was observed in LSF. For PTX-SF-NPs, no obvious peak was detected at around 2θ = 20.19°, which was in accord with FTIR that random coils instead of β-sheets were the conformation of SF in PTX-SF-NPs. The intensive peaks of pristine PTX were not obvious in PTX-SF-NPs, which proved that PTX were encapsulated in the NPs in an amorphous state.

Different from most reported SF NPs and microparticles conformed by β-sheets, the conformation of SF in PTX-SF-NPs was mainly silk I or random coil structure as proved by FTIR and XRD. During the formation of PTX-SF-NPs, hydrophobic PTX played the role of hydrophobic cores of NPs (Scheme 1).

Scheme 1. Schema of PTX-SF-NPs

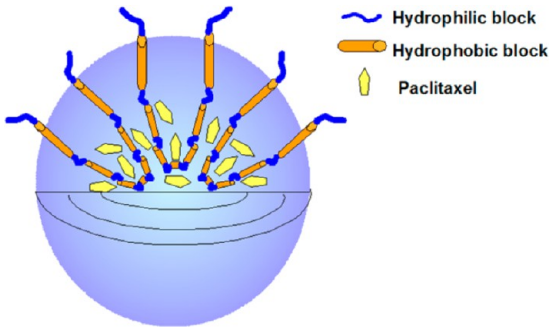

The biopolymer SF, containing both hydrophobic and hydrophilic blocks, self-assembled in the aqueous solution with the hydrophobic core. The hydrophobic blocks were gathered together with PTX, but hydrogen bonds between the hydrophobic repeated amino acid sequences of SF could not formed strongly as the hydrogen bonds in β-sheets. Thus, PTX-SF-NPs with mainly silk I or random coil conformation were formed. As a matter of fact, SF particles with silk I structure fabricated has been reported to show better chemical and physical stability than silk II-rich particles.[14]

3.3. Drug Loading and Release Pattern. The drug loading and encapsulation were assessed by HPLC for three independent batches of NPs. The drug loading and encapsulation efficiency were 10 ± 2% and 52 ± 2%, respectively.

The drug release of PTX-SF-NPs was conducted in a PBS-Tween80 system to enhance the solubility of PTX in water

(Figure 2). A burst release was observed, and 40.9 ± 2.7% of PTX were released in the first 8 h. After that, a steady and

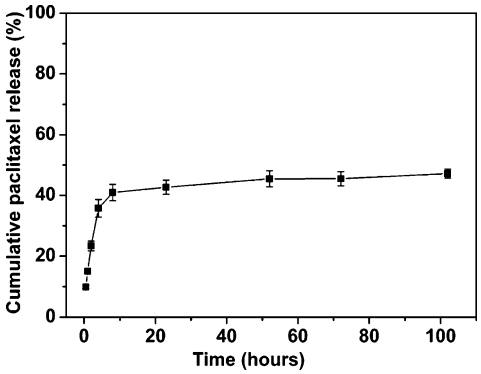

Figure 2. In vitro paclitaxel release from PTX-SF-NPs as a function of time (n = 3).

sustained release was presented with 47.2 ± 1.5% for 100 h. It has been reported that drug release from SF NPs and microparticles was depended on the silk structure and interactions between the compound and silk. In our study, hydrophobic force between PTX and SF was considered to be the major force in NPs without obvious β-sheets formation. The initial burst release was similar to previous reports encapsulating PTX with synthetic biodegradable polymers,[31,32] as the hydrophobic force was the major mechanism for the formation of both PTX polymer NPs and PTX-SF-NPs. Some of encapsulated PTX are located at the hydrophobic–hydrophilic interface inside of the NPs, leading to initial PTX diffusion from the NPs.[33] Another reason is that the release speed is depended on the drug payload and drug density in the NPs, which is higher PTX loading leading to faster release.[33]

3.4. Cellular Uptake of Coumarin-6 Loading Silk Fibroin Nanoparticles. For cellular uptake studies, hydrophobic fluorescein coumarin-6 was selected as model drug to imitate PTX. After incubated with coumarin-6 loaded SF NPs for 2 h, dots of green fluorescence was observed in the cytoplasm and perinuclear space of human gastric cancer cells BGC-823 and SGC-7901, and there was no fluorescence in the nucleus (Figure 3). The phenomenon indicated that drug loading silk NPs could be taken up by gastric cancer cells and accumulated in the cytoplasm and perinuclear space within a short time. The results were in consistent with several other reports that SF particles could be uptake rapidly by cells.[22,34]

3.5. In Vitro Cytotoxicity and Cell Apoptosis Study of Paclitaxel Silk Fibroin Nanoparticles. The in vitro antitumor activity of PTX-SF-NPs against gastric cancer cells was assessed by MTT assay. Regenerated SF aqueous solution was selected as control because its conformation was similar to PTX-SF-NPs as confirmed by FTIR and XRD. PTX-SF-NPs showed comparable cytotoxicity to pristine PTX (Figure 4) in vitro. The cell viabilities of SGC-7901 at 6400 ng/mL equivalent PTX for 48 h were 84.50 ± 14.62% and 76.75 ± 11.45% for PTX and PTX-SF-NPs respectively (Figure 4A). The cell viabilities of BCG-823 at 6400 ng/mL equivalent PTX were 86.69 ± 7.15% and 79.76 ± 8.48% for PTX and PTX-SF-NPs, respectively (Figure 4C). SF showed no cytotoxicity to both kinds of gastric cancer cells even at a high concentration of 2000μg/mL (Figure 4B and 4D). Although the cell viabilities of PTX-SF-NPs group were slightly lower than that of PTX group, no significant difference was obtained.

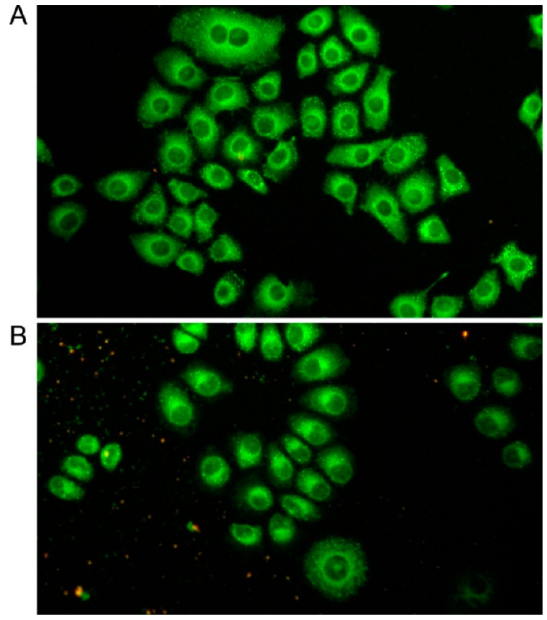

Figure 3. Cellular uptake of coumarin-6 loaded SF NPs by human gastric cancer cells BGC-823 (A) and SGC-7901 (B) (×400).

Because PTX is an anti-microtubule drug and induces cell apoptosis, cell apoptosis studies were investigated with a flow cytometry with PI to stain the dead cells and annexin-V to stain the apoptosis cells. BGC-823 cells were turned round under inverted microscope after being exposed to PTX and PTX-SF-NPs at equivalent dose of 6400 ng/mL for 48h, while the control and SF showed no obvious change in morphology (Figure S1, Supporting Information). The apoptotic cell ratios of control and SF group were 9.8% and 7.5% respectively (Figure 5A and 5B). PTX induced an apoptotic cell ratio of 55.4% (Figure 5C), while PTX-SF-NPs induced 65.6% apoptosis (Figure 5D). Therefore, PTX kept its pharmacological activity after released from PTX-SF-NPs. The preparation process did no harm to the pharmacologically active of PTX.

3.6. In Vivo Antitumor Activity of Paclitaxel Silk Fibroin Nanoparticles. The in vivo antitumor efficacy of PTX-SF-NPs was evaluated on the human gastric cancer BGC-823 nude mice xenograft model (Figure 6). In our study, intraperitoneal injection (ip) of drugs was chosen as the systemic treatment and peritumoral injection (pt) was chosen as the locoregional treatment. The treatments were repeated every four days for three times. Normal saline (NS) and SF solution groups were set as control. It was observed that the growth speed of tumors slowed down on the day after treatment in PTX injection group, PTX-SF-NPs ip and pt group (Figure 6A). However, tumor growth accelerated during the next three days in PTX injection group, and as a result, the tumor growth curve was similar to NS control group. That is because the relative low dose 10 mg/kg was chosen for the study. PTX-SF-NPs ip group showed slower tumor growth and PTX-SF-NPs pt group showed retarding growth or shrink of the tumors. On the Day 13, the relative tumor volumes were 17.77 ±3.71 for PTX injection group, 7.17 ± 0.80 for PTX-SF-NPs ip group (p < 0.05, significantly different from PTX injection group), and 3.91 ± 0.52 for PTX-SF-NPs pt group (p < 0.01, significantly different from PTX injection group; p < 0.01, significantly different from PTX-SF-NPs ip group).

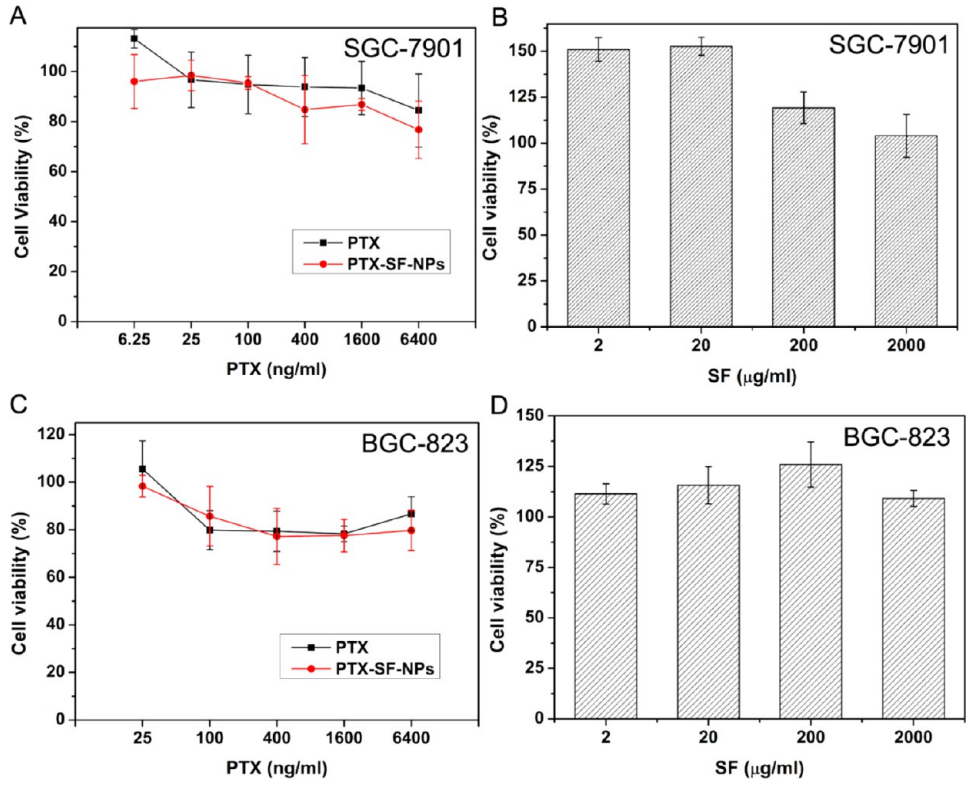

Figure 4. In vitro cytotoxicity studies of PTX-SF-NPs. (A and C) Cell viabilities of BGC-823 and SGC-7901 at different PTX concentrations assessed by 48 h MTT assay. (B and D) Cytotoxicity of SF to BGC-823 and SGC-7901 by 48 h MTT assay.

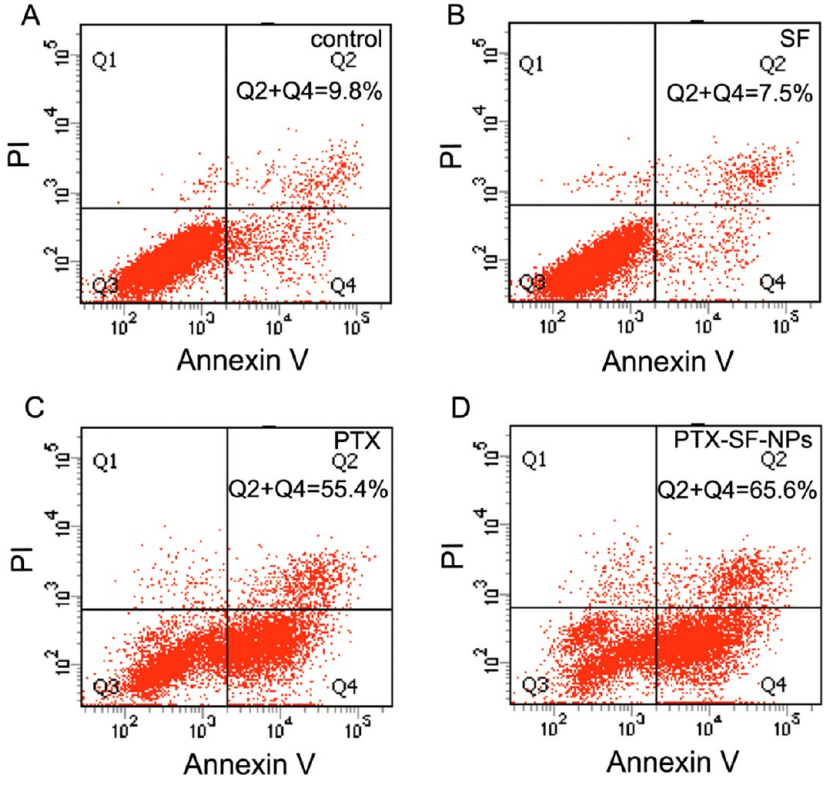

Figure 5. Apoptosis studies of BGC-823 after exposed to PTX or PTX-SF-NPs at 6400 ng/mL PTX for 48 h. Apoptotic cell ratios were calculated by Q2 + Q4.

The absolute tumor weights were recorded and analyzed as a supplement of relative tumor volume. On the Day 14, the mice were sacrificed, and tumors were collected and weighted (Figure 6B). The tumor weights of PTX injection group (0.73 ± 0.17 g) were comparable to that of NS control group (0.70 ± 0.12 g) and SF group (0.85 ± 0.18 g), which was in consistent

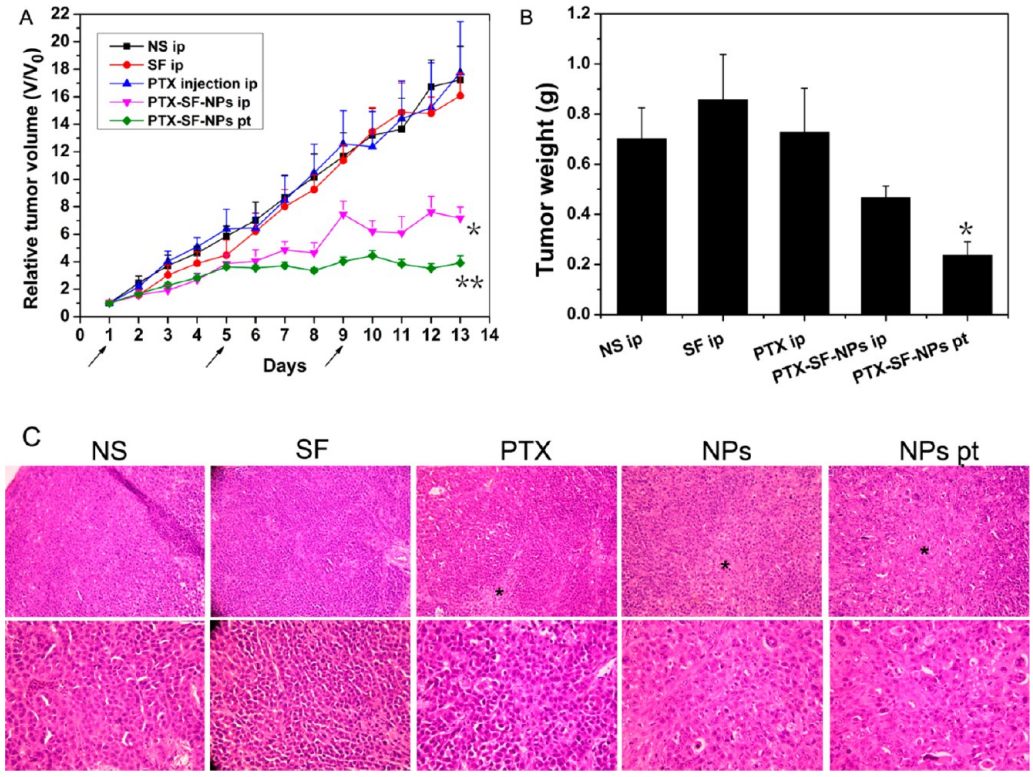

Figure 6. Antitumor efficacies of PTX-SF-NPs for systemic and focal treatment in human gastric cancer BGC-823 nude mice xenograft model. (A) Relative tumor volumes during treatment. Arrows indicate the days treatments were given. The PTX dose was 10 mg/kg for PTX injection ip, PTX-SF-NPs ip, and PTX-SF-NPs pt groups. *, $p < 0.05$ compared with PTX injection group. **, $p < 0.01$ compared with PTX injection group. (B) Absolute tumor weights on Day 14. *, $p < 0.05$ compared with PTX injection group and PTX-SF-NPs ip group. (C) H&E staining of tumors (×200 upper, ×400 lower). *, indicate the necrotic regions.

with the relative tumor volume study. The tumor weights of PTX-SF-NPs ip group (0.47 ± 0.05 g) were lower than PTX injection group although there was no significant difference ($p > 0.05$). The tumor weights of PTX-SF-NPs pt group (0.23 ± 0.05 g) were significantly lower than that of PTX injection group ($p < 0.05$) and that of PTX-SF-NPs ip group ($p < 0.05$).

Pathological studies of the tumors resected on Day 14 were observed via hematein and eosin (H&E) staining of the paraffin embedded tissues (Figure 6C). Crowded tumor cells with large and hyperchromatic nuclei were observed in control group and SF group, and necrotic regions were rare. In PTX injection group, sporadic small areas of pink stained were observed and karyopyknosis in some tumor cells were observed. In PTX-SF-NPs ip group, the discrete necrotic regions were more obvious with cell apoptosis. The phenomena were the most prominent in PTX-SF-NPs pt group, which explained the smallest tumor volumes and lightest weights of the group at pathological level.

For gastric cancer, local recurrence and peritoneal dissemination were the major metastasis and leading cause of death, and locoregional control of disease is important.[24] Meanwhile, SF has been reported well biocompatibility when used locally as regenerative materials. However, few reports have been published on the in vivo experiment of SF NPs for anti-cancer drug delivery, and our study was the first to assess drug loading SF NPs antitumor efficacy in animal models. In the present study, it was proved that PTX-SF-NPs for locoregional treatment showed superior antitumor effect against systemic administration of PTX injection. The EPR effect, high local PTX concentration, controlled release of PTX by NPs, and endocytosis of PTX-SF-NPs are suggested to be the mechanisms of superior anti-tumor effects for systemic and locoregional delivery of PTX-SF-NPs. Although bio-distribution of SF NPs needs to be further investigated, our study confirmed SF NPs as an effective drug carrier for PTX and its enhanced antitumor efficacy by locoregional drug delivery.

In addition, to assess the acute systemic toxicity of PTX-SF-NPs, pathological studies of important organs in each group on Day 14, including hearts, lungs, livers, spleens and kidneys were investigated (Figure S2, Supporting Information). No obvious morphological changes of the organs were found, indicating well biocompatibility and in vivo safety of SF NPs.

CONCLUSION

Biocompatible PTX-SF-NPs were fabricated facilely in aqueous solution without toxic organic solvents and surfactants. Silk I or random coil structure was the main conformation of SF in PTX-SF-NPs. SF NPs could be taken up by human gastric cancer cells and PTX released from PTX-SF-NPs kept its pharmacological activity. Furthermore, PTX-SF-NPs showed superior anti-tumor efficacy for locoregional gastric cancer treatment in vivo. This study highlighted SF NPs as an anti-cancer agent delivery vehicle for locoregional chemotherapy, and its possibility for further clinical application.

ASSOCIATED CONTENT

Supporting Information

Further details of morphological changes of BGC-823 cells after expose to PTX-SF-NPs and H&E staining of organs in animal experiments. This material is available free of charge via the Internet at http://pubs.acs.org.

AUTHOR INFORMATION

Corresponding Author

*E-mail: baoruiliu@nju.edu.cn.

Author Contributions

P.W. and Q.L. contributed equally.

Notes

The authors declare no competing financial interest.

ACKNOWLEDGMENTS

This work was supported by National Natural Science Foundation of China (No. 81172281, 81272741, 81101751, 81302053), Jiangsu Province's Key Medical Center (BL2012001) and the Scientific Research Foundation of Graduate School of Nanjing University (2012CL15).

ABBREVIATIONS

SF = silk fibroin
PTX = paclitaxel
PTX-SF-NPs = paclitaxel-silk fibroin nanoparticles
SFF = silk fibroin fiber
LSF = lyophilized regenerated silk fibroin

REFERENCES

(1) Davis, M. E.; Chen, Z. G.; Shin, D. M. *Nat. Rev. Drug Discovery* **2008**, *7*, 771−782.
(2) Petros, R. A.; DeSimone, J. M. *Nat. Rev. Drug Discovery* **2010**, *9*, 615−627.
(3) Lin, Q.; Li, R. T.; Qian, H. Q.; Wei, J.; Xie, L.; Shen, J.; Yang, M.; Qian, X. P.; Yu, L. X.; Jiang, X. Q.; Liu, B. R. *Biomaterials* **2013**, *34*, 7191−7203.
(4) Lewinski, N.; Colvin, V.; Drezek, R. *Small* **2008**, *4*, 26−49.
(5) Ishida, T.; Harada, M.; Wang, X. Y.; Ichihara, M.; Irimura, K.; Kiwada, H. *J. Controlled Release* **2005**, *105*, 305−317.
(6) Vepari, C.; Kaplan, D. L. *Prog. Polym. Sci.* **2007**, *32*, 991−1007.
(7) Altman, G. H.; Diaz, F.; Jakuba, C.; Calabro, T.; Horan, R. L.; Chen, J.; Lu, H.; Richmond, J.; Kaplan, D. L. *Biomaterials* **2003**, *24*, 401−416.
(8) Omenetto, F. G.; Kaplan, D. L. *Science* **2010**, *329*, 528−531.
(9) Panilaitis, B.; Altman, G. H.; Chen, J. S.; Jin, H. J.; Karageorgiou, V.; Kaplan, D. L. *Biomaterials* **2003**, *24*, 3079−3085.
(10) Wenk, E.; Merkle, H. P.; Meinel, L. *J. Controlled Release* **2011**, *150*, 128−141.
(11) Altman, G. H.; Horan, R. L.; Lu, H. H.; Moreau, J.; Martin, I.; Richmond, J. C.; Kaplan, D. L. *Biomaterials* **2002**, *23*, 4131−4141.
(12) Meinel, L.; Hofmann, S.; Karageorgiou, V.; Kirker-Head, C.; McCool, J.; Gronowicz, G.; Zichner, L.; Langer, R.; Vunjak-Novakovic, G.; Kaplan, D. L. *Biomaterials* **2005**, *26*, 147−155.
(13) Wang, X.; Yucel, T.; Lu, Q.; Hu, X.; Kaplan, D. L. *Biomaterials* **2010**, *31*, 1025−1035.
(14) Lammel, A. S.; Hu, X.; Park, S. H.; Kaplan, D. L.; Scheibel, T. R. *Biomaterials* **2010**, *31*, 4583−4591.
(15) Cao, Z. B.; Chen, X.; Yao, J. R.; Huang, L.; Shao, Z. Z. *Soft Matter* **2007**, *3*, 910−915.
(16) Chen, M.; Shao, Z.; Chen, X. *J. Biomed. Mater. Res., Part A* **2012**, *100*, 203−210.
(17) Shi, P.; Goh, J. C. *Int. J. Pharm.* **2011**, *420*, 282−289.
(18) Bessa, P. C.; Balmayor, E. R.; Hartinger, J.; Zanoni, G.; Dopler, D.; Meinl, A.; Banerjee, A.; Casal, M.; Redl, H.; Reis, R. L.; van Griensven, M. *Tissue Eng., Part C* **2010**, *16*, 937−945.
(19) Zhang, Y. Q.; Shen, W. D.; Xiang, R. L.; Zhuge, L. J.; Gao, W. J.; Wang, W. B. *J. Nanopart. Res.* **2007**, *9*, 885−900.
(20) Zhang, Y. Q.; Wang, Y. J.; Wang, H. Y.; Zhu, L.; Zhou, Z. Z. *Soft Matter* **2011**, *7*, 9728−9736.
(21) Zhu, L.; Hu, R. P.; Wang, H. Y.; Wang, Y. J.; Zhang, Y. Q. *J. Agric. Food Chem.* **2011**, *59*, 10298−10302.
(22) Kundu, J.; Chung, Y. I.; Kim, Y. H.; Tae, G.; Kundu, S. C. *Int. J. Pharm.* **2010**, *388*, 242−250.
(23) Wolinsky, J. B.; Colson, Y. L.; Grinstaff, M. W. *J. Controlled Release* **2012**, *159*, 14−26.
(24) Hartgrink, H. H.; Jansen, E. P. M.; van Grieken, N. C. T.; van de Velde, C. J. H. *Lancet* **2009**, *374*, 477−490.
(25) Sakamoto, J.; Matsui, T.; Kodera, Y. *Gastric Cancer* **2009**, *12*, 69−78.
(26) Weiss, R. B.; Donehower, R. C.; Wiernik, P. H.; Ohnuma, T.; Gralla, R. J.; Trump, D. L.; Baker, J. R.; Vanecho, D. A.; Vonhoff, D. D.; Leylandjones, B. *J. Clin. Oncol.* **1990**, *8*, 1263−1268.
(27) Gelderblom, H.; Verweij, J.; Nooter, K.; Sparreboom, A. *Eur. J. Cancer* **2001**, *37*, 1590−1598.
(28) Rockwood, D. N.; Preda, R. C.; Yucel, T.; Wang, X. Q.; Lovett, M. L.; Kaplan, D. L. *Nat. Protoc.* **2011**, *6*, 1612−1631.
(29) Laemmli, U. K. *Nature* **1970**, *227*, 680−695.
(30) Zhou, C. Z.; Confalonieri, F.; Jacquet, M.; Perasso, R.; Li, Z. G.; Janin, J. *Proteins: Struct., Funct., Genet.* **2001**, *44*, 119−122.
(31) Zhu, Z. S.; Li, Y.; Li, X. L.; Li, R. T.; Jia, Z. J.; Liu, B. R.; Guo, W. H.; Wu, W.; Jiang, X. Q. *J. Controlled Release* **2010**, *142*, 438−446.
(32) Li, X. L.; Lu, X. W.; Xu, H. E.; Zhu, Z. S.; Yin, H. T.; Qian, X. P.; Li, R. T.; Jiang, X. Q.; Liu, B. R. *Mol. Pharmaceutics* **2012**, *9*, 222−229.
(33) Chen, H. T.; Kim, S. W.; Li, L.; Wang, S. Y.; Park, K.; Cheng, J. X. *Proc. Natl. Acad. Sci. U. S. A.* **2008**, *105*, 6596−6601.
(34) Gupta, V.; Aseh, A.; Rios, C. N.; Aggarwal, B. B.; Mathur, A. B. *Int. J. Nanomed.* **2009**, *4*, 115−122.